Proceedings of ASME Turbo Expo 2020
Turbomachinery Technical Conference and Exposition
GT2020
September 21-25, 2020, London, England

GT2020-16040

DESIGN SPACE EXPLORATION OF TURBINE BLADE SHROUD INTERLOCK FOR FLUTTER STABILITY
(ACCEPTED MANUSCRIPT)

Olatz Larrieta[1,3], Roberto Alonso[1], Óscar Pérez Escobar[2], Ibrahim Eryilmaz[3], Vassilios Pachidis[3]

[1]ITP Aero, Zamudio, Bizkaia, Spain
[2]ITP Aero, Alcobendas, Madrid, Spain
[3]Cranfield University, Bedfordshire, UK

ABSTRACT

The geared turbofan engines bring the potential to rotate the fan at lower speed and allow an increase in diameter, which in turn leads to an increase in propulsive efficiency through high by-pass ratio. The low-pressure turbine stages driving the fan can also rotate at high speed resulting in fewer stages when compared to traditional turbofans. However, when operating at high speed, pressure fluctuations due to self-excited vibrations increase and may provoke flutter instabilities.

In a geared architecture, to deliver the high power required by the fan and the intermediate-pressure compressor, the low-pressure turbine system operates at higher temperatures compared to its predecessors. This phenomenon requires structural materials with higher heat resistance, which carries the inconvenience of poor welding suitability. That is the reason why alternative non-welded blade shroud joint techniques are so important, techniques as the blade interlock mechanism studied in this work.

This manuscript examines the effects of different design parameters of a low-pressure turbine blade shroud interlock on flutter stability, to make future recommendations for geared engines. The shrouded turbine rotor blades feature blade interlocks, which enhances the dynamic stability by providing stiffness to the rotor blade row. To assess the stability of the system, a parametric design of a turbine blade-disk assembly was prepared. In the parametric model the design variables that define the blade interlock are the interlock angle, interlock axial position, interlock contact length and height, knife seal position and pre-twist angle.

After parametrization, a finite element model of the turbine blade and disk assembly was prepared with cyclic symmetry boundary condition. The stresses caused by rotation were calculated in a static structural analysis and these were used as pre-stress boundary conditions in modal analysis. The modal results were afterwards exchanged with an aerodynamic model to obtain the aerodynamic damping for different blade interlock design configurations.

In the present work, the dynamic response of the first three excitation modes was analyzed. It was found that the third mode was stable for all the design points, whereas first and second modes were unstable at least for the reference design point. Among the considered six different parameters that define the blade interlock geometry, the interlock contact position turned to be the most influential parameter for modal response and for flutter stability. Moving the interlock contact position towards the trailing edge gave the most beneficial results. On the other hand, the interlock angle showed the least influence on both, the modal analysis and flutter behavior. The accomplished Design of Experiments and subsequent optimization process also conclude that there exists an interdependency between the studied parameters.

Keywords: Blade Interlock, Dynamic Analysis, Flutter Stability

NOMENCLATURE

2D	2 Dimensional
3D	3 Dimensional
ACARE	Advisory Council for Aviation Research and Innovation in Europe
CAD	Computer Aided Design
CFD	Computational Fluid Dynamic
DoE	Design of Experiments
DP	Design Point
EU	European Union
FEM	Finite Element Method
HPC	High Pressure Compressor
HPT	High Pressure Turbine
IBPA	Interblade Phase Angle
IPC	Intermediate Pressure Compressor
IPT	Intermediate Pressure Turbine

ITP	Industria de TurboPropulsores
LPT	Low Pressure Turbine
ND	Nodal Diameter
nm	Nautical Miles
PS	Pressure side
RANS	Reynolds Averaged Navier-Stokes
rpm	Revolution per minute
SS	Suction side
UPD	Under-platform Dampers
XWB	Extra Wide Body
A	Interlock Axial Position
B	Knives Position
C	Interlock contact Length
c	Objective Function
D	Interlock Contact Length
E	Modulus of Elasticity
x	Vector of Design Variables
α	Thermal Expansion Coefficient
ρ	Density
υ	Poissons's Ratio

INTRODUCTION

Gas turbine engines have progressively evolved during the last decades towards more efficient fuel consumption systems, in line with the targets of ACARE EU Flightpath 2050 [1]. To that end, aircraft engine manufactures are investing considerable amount of budget and resources in improving the performance of their products with the challenge of getting highly efficient, environmentally friendly, light-weight and low-cost turbomachines. Two development programs namely the Safran Ultra-High Propulsive Efficiency engine and the Rolls-Royce UltraFan™ engine target to increase the propulsive efficiency through increasing engine by-pass ratio. Therefore, the thrust generation relies on passing higher mass flows through the fan rather than generating thrust through the core [2–4]. When the Rolls-Royce Trent XWB direct drive architecture is compared with the Rolls-Royce UltraFan™ geared architecture, the design changes from 1 Fan, 8 IPC, 6 HPC, 1 HPT, 1 IPT and 6 LPT stages to 1 Fan, 3 IPC, 9 HPC, 2 HPT and 4 combined IPT-LPT stages. In the geared turbofan, the HP system is longer, the combined IPT-LPT directly drives the IPC and drives the fan by a reduction gearbox. The reduction is necessary to mitigate excessive fan shock losses due to the very large fan diameter. Therefore, the combined IPT-LPT system rotates faster when compared to the LP system of a direct drive [5]. Considering that modern LPTs entail 15% of the total costs and contribute 20% of the total weight of the turbomachinery [6], geared architectures offer cost reductions due to reduction in the stage count. Bijewitz et. al carried out a comparative study between a direct drive and a geared drive turbofan for a 4800nm, 340 passenger, 2035+entry wide body aircraft [7]. Additional to the reduced fuel burn, they reported that despite the component count reduction, there is not a significant decrease in the overall engine weight in the geared drive turbofan when compared to a direct drive. The combined IPT- LPT system driving the fan and the IPC is characterized by higher rotational speed, low stage count and less manufacturing and maintenance costs.

In this manuscript the combined IPT-LPT system is named as LPT and flutter behavior of a LPT blade is investigated as these blades are prone to flutter.

Flutter is a self-induced vibration that occurs when a supported surface is bent under an aerodynamic excitation. This aeroelastic phenomenon may appear as a "buzzing" in the structure of the plane (which is the less hazardous form), but can also uncontrollably fail at high speed. That is why, among the different phenomena that affect the turbomachine's blade mechanical integrity, flutter analysis in LPTs has become a prime concern with research being carried out to get a deeper understanding and to find the most important contributors to the flutter phenomenon. The most relevant variable to predict flutter is the mode shape followed by the frequency value [8,9].

Designers endeavor to design "flutter-free" blade assemblies and focus on modifying the geometry in order to improve the vibration frequency and mode shapes. A quite expanded way to improve the dynamic behavior of the system is by increasing the structural damping using shrouded blades [10].

Among the different alternatives to control the vibration of shrouded LPT blades, one can find the following solutions: cantilevered blades, welded-in-pairs rotor blades and blades with interlock unions (see Figure 1) [11]. The cantilever solution shows little control over the vibration of its flat-sided shrouds, especially if low interblade phase angles (IBPA) are considered. An alternative to the latter is the use of in-pair-welded blades. These are a pair of blades which are joined at their shrouds with a weld enhancing the structural stiffness of the assembly. This set up exhibits lightly modified mode shapes and frequencies in comparison with the cantilever type. Another alternative to the latter is the Z shaped shrouds used in interlock systems.

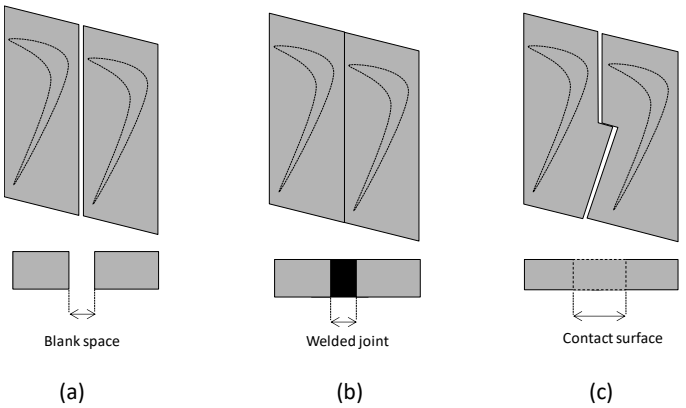

FIGURE 1: BLADE SHROUDED VIBRATION CONTROL SOLUTIONS: a) CANTILEVER BLADE, b) IN-PAIR-WELDED BLADES AND c) BLADES WITH INTERLOCK CONFIGURATION

This latter approach is based on the creation of a contact surface that is pre-stressed in order to assure the contact and, at the same time, to minimize wear. The pre-stress force guarantees the connection between blades also in a cold ambient and at low speed. The Z shaped shrouded blades shown in Figure 1c

maintain a pre-load along the circumference while performing the function of sealing [12]. In addition, the blade interlock mechanism is also a good design alternative to welded blades as difficult-to-weld superalloys like INCONEL718, CMSX-4 or UDIMET may exhibit cracking tendencies in welding during first time fabrication and repair. Near the welding heat affected zone, material properties can change significantly [13–15].

However, blade interlock systems may lead to complex mode shapes, since the mode shapes can fiercely vary with the nodal diameter. Therefore, this type of blade shroud significantly alters the mode shapes and frequencies of the previously proposed solutions. In what concerns the aerodynamics, this alteration is nonetheless beneficial since it raises the frequency of the assembly [11].

The present work falls within the scope of understanding and optimizing the blade interlock mechanism to improve the dynamic behavior of the assembly, mainly focusing in flutter stability. To that end, this work evaluates the aerodynamic damping. The study and obtained results will form the fundamentals of future blade design processes.

Through application of CAD, FEM and CFD, a DoE has been implemented to identify the interdependencies between aeroelastic behavior and geometric parameters. Based on the database obtained from the DoE, a best-case design set is obtained that can offer design recommendations on blade interlocks.

1 METHODOLOGY

The modelling and simulation provide the opportunity to imitate the real working conditions at low cost. Viable design concepts can be obtained from a large design space and the modelling can also support the experimentation process. In order to evaluate the dynamic behavior of a blade and disk assembly and see the influence of the blade interlock contact design in flutter analysis the steps shown in the methodology chart (Figure 2) were followed.

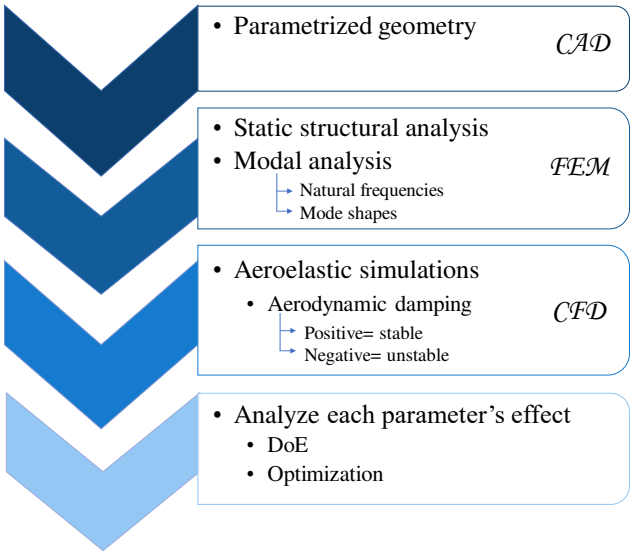

FIGURE 2: PROCESS FLOWCHART

The process started by building a parametrized CAD model in NX. Based on the parametrized geometry, a DoE set was prepared. The dynamic behavior of each design set was analyzed using a finite element method, by means of ANSYS Workbench, considering the in-flight operating conditions. For that end, a static structural analysis was used as an input for the next modal analysis. The mode shapes and frequencies obtained from this latter analysis were used as the input data for the subsequent aeroelastic behavior simulation using an internally developed CFD software to obtain the aerodynamic damping. This method was repeated for every design point considered in the DoE. And after the assessment of the results, relations within the design parameters were obtained and the best case was identified for flutter stability.

1.1 Geometry definition and identification of the parameters

The first step towards achieving an optimum solution by Design of Experiments, is to build a parametric model of the geometry to be analyzed. The CAD model built for this project was a highly parametrized blade geometry. However, considering that the present work was focused on the optimization of the interlock, the parameters corresponding to the airfoil or the bottom of the blade were set as fixed parameters in order to simplify the calculation process.

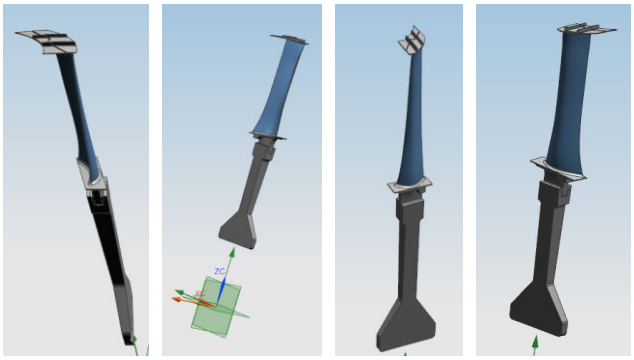

FIGURE 3: CAD MODEL WITH PARAMETRIZED BLADE SHROUD

The starting model (Figure 3) was a blade and disk assembly with interlock contact of a geared turbofan LPT. The goal was to check whether the dynamic response of the blade could be improved by changing the considered parameters. For that reason, the CAD model was built with the capability of adapting its geometry when any of the considered parameters listed below were modified (see Figure 4):

- **Interlock angle**: it refers to the angle of the interlock contact in the tangential direction.
- **Interlock position**: it refers to the axial position of the contact with respect to the middle of the shroud. This parameter is associated with the change of the center of gravity location.
- **Interlock contact length**: it refers to the contact length of the assembly (axial and tangential direction).
- **Interlock contact height**: it refers to contact height of the assembly (radial direction).

• **Knives position**: it is the relative axial position of the knives referred to the contact.
• **Pretwist angle**: it refers to the shroud pretwist to generate the geometric interference. This parameter guarantees an unceasing force presented between two adjacent blades during all the operating conditions. Therefore, an increase of the pretwist angle results in an increase in the total contact pressure, whereas an excessively small value might not assure the contact in all the conditions.

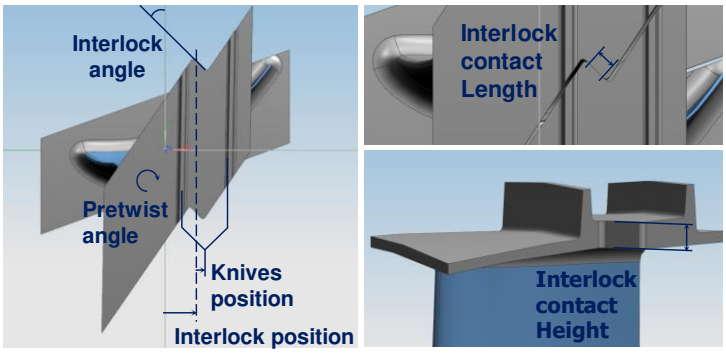

FIGURE 4: LOCATION OF THE CONSIDERED PARAMETERS

The upper and lower limits of the shroud interlock parameters, given in Table 1, were used in the DoE study.

TABLE 1: RANGE OF THE PARAMETERS

	Max	Nominal	Min
Interlock angle (º)	60	45	30
Interlock position (mm)	7.0	0.0	-7.0
Interlock contact Length (mm)	5.0	3.0	1.0
Interlock contact Height (mm)	4.0	2.5	1.5
Knives position (mm)	2.0	0.0	-2.0
Pretwist angle (º)	1.5	1.0	1.0

1.2 Finite Element model

Once the geometry and the parameters were defined, to quantify their effect in the dynamic behavior of the assembly, the next procedure was followed by all the design points. To that end, the process is only explained for the DP0, which was considered as the nominal design point and is imitated for the rest of DPs (Design Points).

Ni-based alloys were used in this problem and these materials' details are defined, as shown in Table 2, where Young modulus (E), Poisson coefficient (ν), density (ρ), and thermal expansion coefficient (α) are provided.

TABLE 2: MATERIAL PROPERTIES

	E (GPa)	ν	ρ (kg/m^3)	α (10^{-5}°C^{-1})
Blade	170	0.30	8300	1.35
Disk	180	0.30	8100	1.45

Evaluating the modal response of an assembly does not require a highly refined mesh, therefore the domain was discretized with around 400k tetrahedron elements (600k nodes). In addition, the case in hand allows to define a cyclic symmetry, which does in turn significantly diminish the computational cost since it is only necessary to define one cyclic portion to construct the full response.

For a realistic representation of the system, two contacts were defined: the disk-blade bonded union and a frictionless contact between blades. The non-linearity of the contact is considered for the static analysis, while for the modal simulations, the fixed contact condition was applied for the already calculated contact surface. The boundary conditions were also in line with the engine operating conditions as illustrated in the Table 3.

1.3 FEM and CFD simulations

As explained before, using finite element analysis a static structural simulation was first run which provided the input for the subsequent pre-stressed modal analysis. The first three modes obtained from the latter were then studied for each of the DPs, considering different nodal diameters. The resulting data

TABLE 3: BOUNDARY CONDITIONS

Boundary conditions	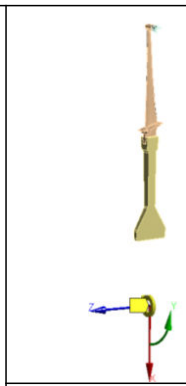	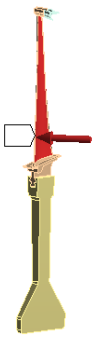	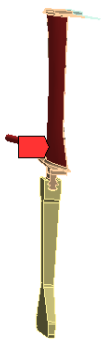		
	Rotational speed (rpm)	Pressure on PS (MPa)	Pressure on SS (MPa)	Blade Temperature (ºC)	Disk Temperature (ºC)
Value	9000	0.20	0.12	650	500

(frequencies and mode shapes) were then used for a flutter behavior evaluation by means of computational fluid dynamic analyses.

Flutter analysis were performed using a linearized un-coupled methodology as described in [11]. This methodology assumes that the effects of the aerodynamics on structural modal shapes and natural frequencies is negligible, so natural frequencies and modal shapes were obtained as explained in the previous section ignoring aerodynamics effects.

The CFD flutter solution can be decomposed into a mean or steady flow plus a small periodic perturbation.

Steady flow was computed using the in-house CFD solver called Mu^2s^2T, developed at ITP Aero. Mu^2s^2T solves the 3D RANS equations in relative reference frame. In these simulations unstructured grids were used to discretize the fluid domain and variables were stored at cell vertex points. Mu^2s^2T allows the use of a fully implicit Jacobi solver or an explicit five-stage Runge-Kutta scheme for time integration. Besides, turbulence can be modelled either with algebraic Baldwin-Lomax eddy viscosity model or Wilcox's two equation k-ω model.
The linearized solver Mu^2s^2T-L calculates the unsteady linearized solution, for which similar algorithms to the steady solver are employed to maintain the consistency between solutions. In the linear solver structural displacements are interpolated and imposed on the aerodynamic mesh to determine the work per cycle and the aerodynamic damping. Effectiveness and robustness of the used solver can be found in [16–18], where the extended code is explained and the validation of the simulations are proven by comparing the computational results with the experimental ones.

1.4 Results and data treatment

In the study, a superficial broad-range DoE was taken as reference for a subsequent more precise DoE. The initial DoE was useful to identify those parameters that are more dominant while a more refined DoE is needed to analyze the interaction and sensitivity of the chosen parameters. Once all the results of both DoE were obtained, they were treated using statistical tools. In the end, an optimization process was carried out in order to obtain the best configuration.

2 DESIGN OF EXPERIMENTS

2.1 Parameters selection

In order to analyze the influence of each parameter (defined in section 1.1) in the dynamic response of the total assembly and define a more precise subsequent DoE, the modal and aerodynamic simulations of different design points were developed. This research has analyzed the dynamic response of the first three modes. However, the third mode was stable for all the considered design points, with values of aerodynamic damping coefficient ranging from 0.01-0.66%. So, as the target was to improve the dynamic response of the assembly by obtaining a flutter-free blade-disk configuration, no further analysis was considered necessary for this already stable third mode. Overall, this work focused only on the response of the first and second modes.

Firstly, the aforementioned nominal configuration (see Table 1) was run, which was used as a reference for the following evaluations. The results were obtained for harmonic indexes, also known as nodal diameters, from 8 to 24 and for both vibration modes. Figure 5 shows in each column the natural frequency results and the corresponding aerodynamic damping coefficient for the first and second modes for the reference configuration. An increase in the nodal diameter usually implies a non-linear increase in the natural frequencies. However, taking into account the system's aerodynamic stability there is no such clear relation. In fact, the following conclusions can be obtained from the plots that are in the second row of Figure 5. The aerodynamic damping coefficient of positive nodal diameters turned to be positive, which means that all the positive harmonic indexes will contribute towards a flutter stable situation by enhancing the aerodynamic damping of the system. However, some responses of negative nodal diameters are below the dashed line. This dotted line represents the limit between stable and unstable aerodynamic damping. Therefore, for flutter-free configuration all the results should be above that line. In Figure 5, the most unstable situation was marked, 24ND for the first mode and 16ND for the second mode, in which the smallest aerodynamic damping coefficients were obtained. Even though all the nodal diameters for all the design points were simulated, for simplicity only the ones corresponding to these extreme nodal diameters are displayed in the following lines, because in general, increasing the aerodynamic damping of the less stable situation improves the aerodynamic behavior of the entire assembly. Figure 6 displays the mode shape results for the aforementioned first and second mode responses.

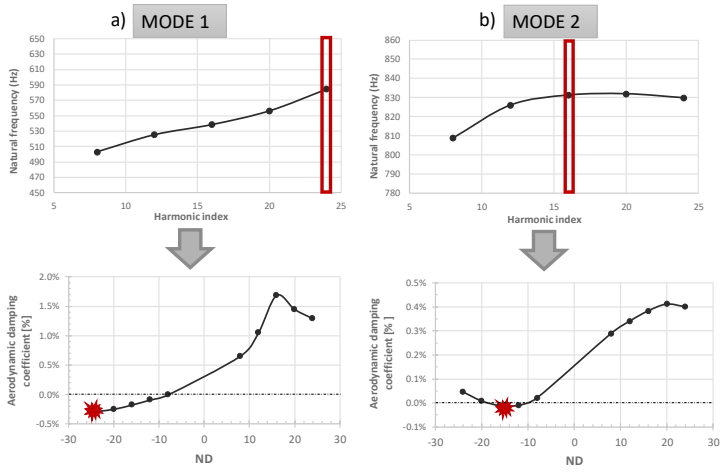

FIGURE 5: MODAL AND AERODYNAMIC RESULTS FOR THE a) FIRST MODE AND b) SECOND MODE

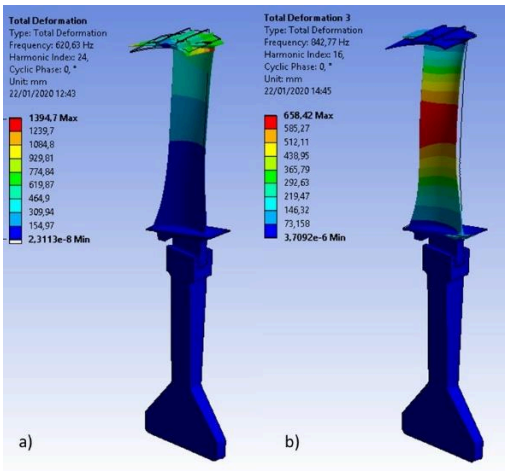

FIGURE 6: MODE SHAPES FOR a) FIRST MODE AND b) SECOND MODE

For the best selection of the parameters, the first and second modes are individually analyzed, since their responses are not related (see Figure 5). Taking into account just the results for the nodal diameter number 24 and the first mode, Figure 7 and Figure 8 are obtained.

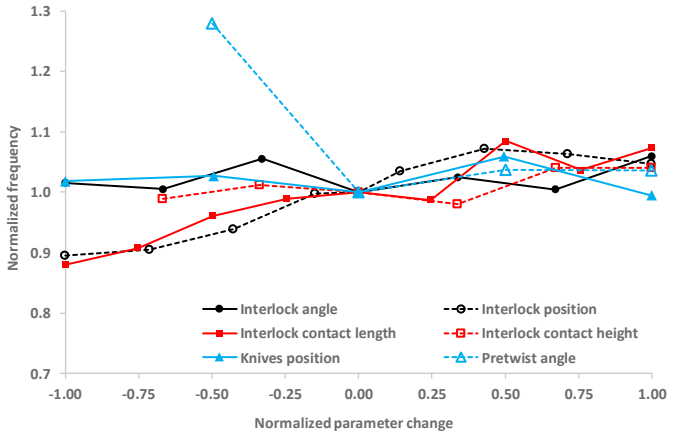

FIGURE 7: PARAMETER CHANGE INFLUENCE IN THE NORMALIZED NATURAL FREQUENCY VALUE FOR THE FIRST MODE.

Figure 7 displays the natural frequency results for different values of the interlock angle, interlock position, interlock contact length, interlock contact height, knives position and pretwist angle. The data was provided considering 0 as the nominal parameter value and 1 and -1 refer to the maximum and minimum values respectively that these parameters received (see Table 1). It was concluded from the results that there is no repetitive tendency between the obtained values. The pretwist angle's modal frequency increases drastically when its value is below the nominal value. That is because, when contact is not assured (small pretwist angle values) the contact face is reduced and therefore the design becomes less rigid. This rigidity decrease will create a completely different behavior. On the other hand, the other two parameters that show a more relevant increase when the value of the parameter is increased are the interlock position and the interlock contact length.

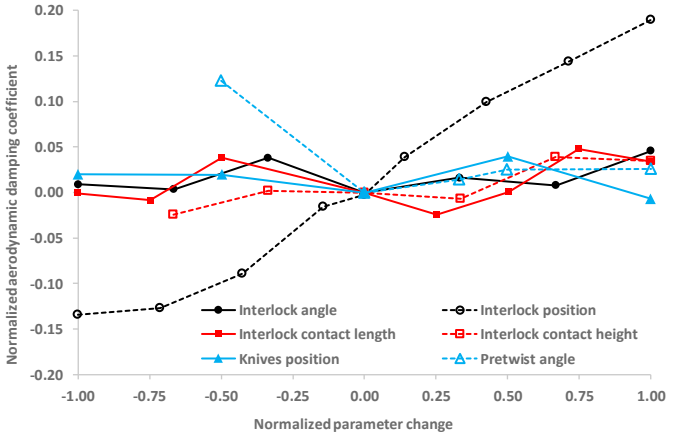

FIGURE 8: PARAMETER CHANGE INFLUENCE IN THE NORMALIZED AERODYNAMIC DAMPING COEFFICIENT FOR THE FIRST MODE.

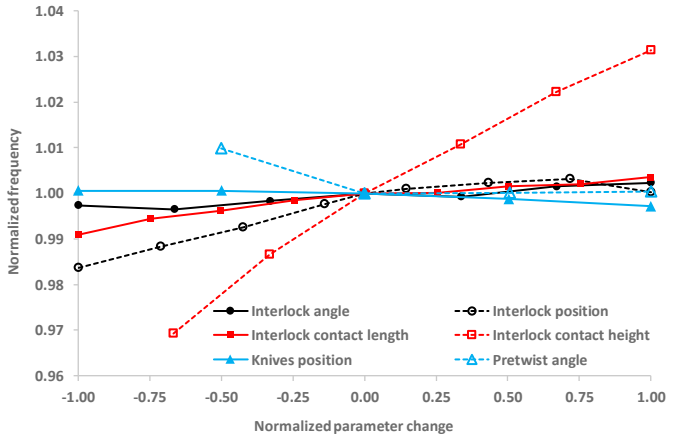

FIGURE 9: PARAMETER CHANGE INFLUENCE IN THE NORMALIZED NATURAL FREQUENCY VALUE FOR THE SECOND MODE.

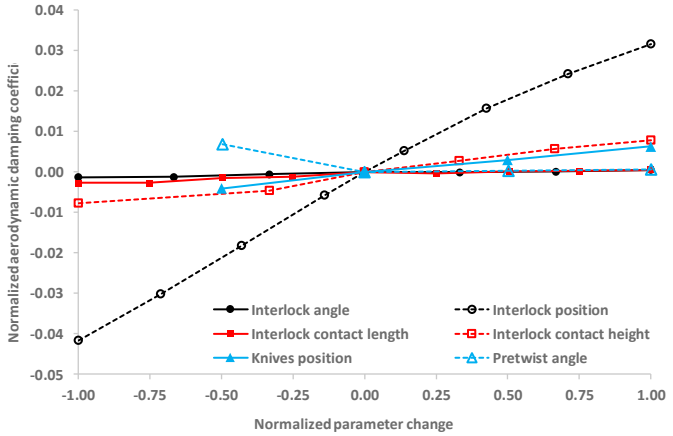

FIGURE 10: PARAMETER CHANGE INFLUENCE IN THE NORMALIZED AERODYNAMIC DAMPING COEFFICIENT FOR THE SECOND MODE.

Figure 8 represents the aerodynamic damping coefficient values for the same design points considered in Figure 7. The results show clearly that the interlock position is the parameter that most significantly improves the aerodynamic damping of the system.

After obtaining the frequencies and stability results for the first mode, the same procedure was followed for the second mode, but in this case instead of 24ND, the 16ND was taken into consideration. Figure 9 and Figure 10 show the system's natural frequency values and the aerodynamic damping coefficients respectively.

According to Figure 9 and Figure 10, the variation for the second mode is less evident than for the first mode, and each parameter's variation entails less influence in modal and aerodynamic responses. Furthermore, the system seems to be more stable, and in some configurations, a flutter-free design for the second mode can be achieved. Even though there is less variation between the maximum and minimum frequencies and aerodynamic damping coefficients, the most remarkable parameter is still the interlock position.

In short, taking the first and second modes' analysis into consideration it was concluded that on the contrary to what it was predicted, interlock angle showed almost no influence at all neither in the modal analysis nor in the flutter behavior. This is due to the fact that modal analysis considered tied interlock interfaces, but the tied area depends on the contact status calculated during the non-linear static analysis. Interlock angle could have affected the static condition (like contact area) and its effect could have changed modal response. However, changes in contact due to the angle are small, and consequently it has nearly no effect on flutter stability.

In addition, since a contact face increase raises the rigidity of the system, usually it also improves flutter stability. For the interlock contact length and contact height effect in flutter analysis, interlock contact length was quite relevant as its value fluctuates higher when compared to contact height around the zero y-axis value of Figure 8 as a function of the parameter change span. On the other hand, according to their deviation from the zero y-axis value of the Figure 9, the interlock contact height was more influential than the contact length for the second mode. This is more visible in the statistical analysis given in Figure 12. However, when compared to the dominant influence of the interlock axial position, contact height and contact length can be considered to have the similar influence.

For pretwist angle two differentiated responses were found. When contact is assured, that is when the pretwist angle takes values higher than or equal to unity, the parameter does not have a large influence in any of the analyses. On the other hand, when working with too small pretwist angles the contact face is reduced and therefore the design becomes less rigid. This rigidity decrease will create a different behavior in the modes. In this case, the effect was unfavorable for the first mode because even though the modal and aeroelastic results were improved for the presented 24ND; the response of the rest of the NDs change abruptly. Therefore, the worst case for the first mode appeared at a different ND value and with an aerodynamic damping value lower than the reference one.

Among all the considered parameters, the interlock axial position with respect to the middle of the shroud turned out to be the most relevant parameter for both, modal and flutter analyses and both first and second modes. Indeed, moving the interlock contact towards the trailing edge gave the most beneficial results. Lastly, the effect of the knives position can be considered almost null for improving the flutter response of the assembly. Nevertheless, a possible interdependency between the mentioned last two parameters is expected, that is why for the next calculations this effect was not neglected.

2.2 Parameters sensibility

Based on the previous DoE results, a refined Design of Experiments was carried out taking into account the most relevant 4 parameters and reducing the parameters' range to the most appropriate. For this analysis a linear behavior between the parameters and the results was also assumed.

For the accomplishment of this work only the interlock axial position, knives position, interlock contact length and interlock contact height were taken into account, and a DoE of 16 different design points was run in order to verify the full response of the assembly.

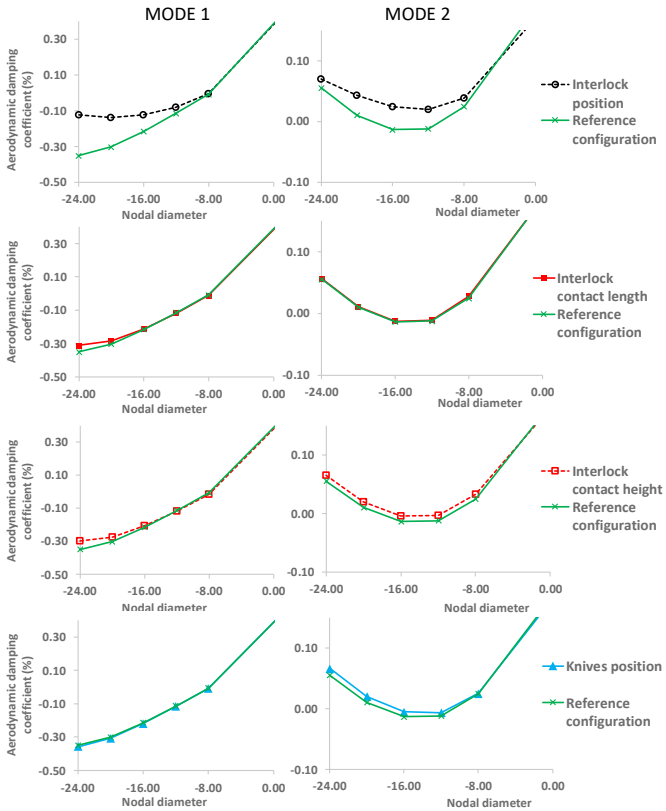

FIGURE 11: AERODYNAMIC STABILITY RESULTS FOR THE CONSIDERED FOUR PARAMETERS FOR FIRST MODE (first column) AND SECOND MODE (second column)

Figure 11 displays the most relevant plots to see the individual effect of the parameters on flutter stability for both

modes, where the abscissa refers to the nodal diameters and the ordinate represents the aerodynamic damping coefficient of each of the considered points. In the first row the influence of the interlock axial position is given, which represents by far the most remarkable effect in flutter. The following three rows are referred to the responses for the knives position and interlock contact length and height which create some significant changes in the aerodynamic damping results. Taking all these results into account and treating them statistically, the pareto diagrams of standardized effects were obtained (see Figure 12). The pareto diagram shows the individual effect of each parameter and the combined effect of the multiple parameters on the aerodynamic damping coefficient. In this case, as mentioned before, the evaluation was focused on the ND24 for the first mode and in the ND16 for the second one.

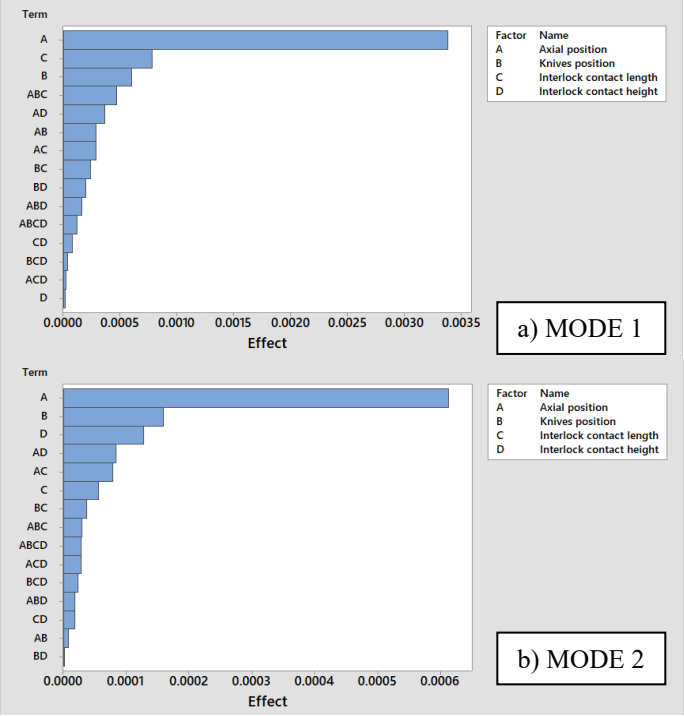

FIGURE 12: PARETO DIAGRAMS FOR a) FIRST MODE and b) SECOND MODE

This analysis suggested that when modifying each parameter, the effect is considerable, but that effect is different for the first and second mode of frequencies (Figure 12 a and b respectively). As it was foreseen, the interlock axial position turned out to be the most relevant parameter for both vibration modes. Apparently, the knives position has also an undoubtable effect in both configurations even though this was not completely in line with the previous DoE. In addition, the assumption that the interlock contact length is more relevant for first mode, while the interlock contact height plays a crucial part in the second one, was again confirmed. These results also verify that there exists an interdependency between the parameters but its effect is minimal in comparison to the effect of each parameter individually.

3 OPTIMIZATION

This last part of the work proposes an optimum design point for a blade-disk system, based on the previous statistical analysis.

The flutter stability of the blade-disk system is measured as an aerodynamic damping coefficient, which can be positive or negative, making the system stable or unstable, respectively. As the unstable situation can lead to blade damage due to flutter, the objective function is defined as the absolute value of the aerodynamic negative damping (see equation 1).

$$\begin{aligned} &minimise\ c(\boldsymbol{x}) \\ &\boldsymbol{x} \in \mathbb{R} \end{aligned} \tag{1}$$

where c is the objective function and $\boldsymbol{x}$ is the vector of the design variables, that must be inside the real domain $\mathbb{R}$.

The optimization process focusses on the behavior of the first two vibration modes since third mode is completely stable for any of the considered design points.

The optimization has the same conditions as before in terms of boundary conditions and only concentrates on selected design variables for a better stability condition. The vector of design variables, **x**, is composed of the values of the four most relevant parameters that define the blade interlock geometry: interlock position, interlock contact length, interlock contact height and knives position.

The optimization problem is finally defined as the iterative process of finding the design variable vector that, without violating the pre-established design constraints, minimizes the value of the objective function [19], in this case, the absolute value of the aerodynamic negative damping. This value of the objective function is representative of the response of the design.

The optimization process is explained in the following lines. First, an initial set of design variables is defined along with the initial reference values. Second, a complete finite element analysis and aeroelastic analysis is performed to compute the value of the objective function with the present variables value. Third, a parameter is selected and its value is varied while the rest of the parameters' values remain equal. Fourth, a new complete analysis is performed for the new set of parameters. Step 3 and 4 are repeated until the entire range of Table 1 is covered and the objective function for each combination of the parameter's redefinition is obtained. The optimum result will then be given by the set of values that give the global minimum of the objective function. It was concluded that the best configuration was obtained for the considered maximum interlock position and interlock contact and minimum knives position, as in Table 4.

TABLE 4: REFERENCE AND OPTIMUM DESIGN PARAMETER'S VALUES

	Reference	Optimum
Interlock position (mm)	0	7
Interlock contact Length (mm)	3	5
Interlock contact Height (mm)	2.5	4
Knives position (mm)	0	-2

In order to see the effect that the optimum configuration shows in comparison to the nominal or reference situation, Figure 13 and Figure 14 are provided for the first and second modes respectively. These figures represent the normalized aerodynamic damping coefficient in the ordinate axis for each of the considered nodal diameters depicted in the abscissa axis.

3.1 First excitation mode

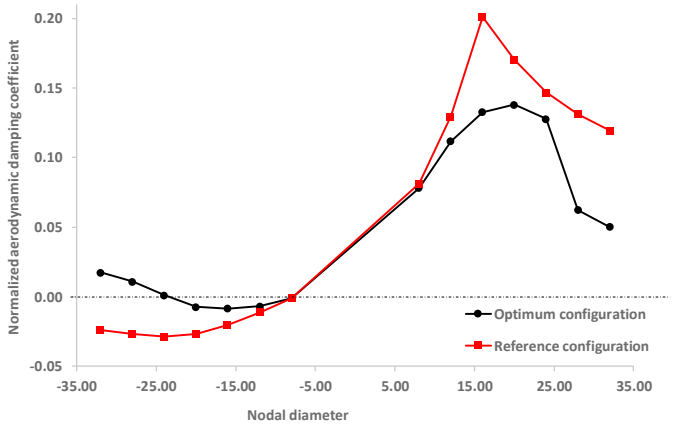

FIGURE 13: NORMALIZED FLUTTER STABILITY RESULTS FOR THE FIRST EXCITATION MODE – NOMINAL AND OPTIMAL CONFIGURATIONS

Regarding the response for the first excitation mode it can be concluded that all the absolute values of the aerodynamic damping coefficients are reduced. Despite the reduction, the positive nodal dimeters are still stable but the unstable negative diameters become stable except in a certain region, see Figure 13. In general, the first mode's stability is quite improved in comparison to the reference design point; however, there are still some negative aerodynamic damping values. Even though the considered 24ND has turned into positive, the ND 20 and 16 are still under the stability line limit. Therefore, in terms of aerodynamic damping this optimum configuration cannot ensure a flutter-free design unless a sufficient structural damping is inserted. Structural damping is always positive and will depend on blade connections, materials and ND [8,12]. If the aerodynamic damping that results from the calculations is negative and exceeds the available structural damping of the component, flutter will occur. In order to avoid flutter a full response analysis is needed as both aero damping and structural damping values are required. If the total damping coefficients is still negative, some extra devices such as friction dampers can be used. The most commonly used friction device is the under-platform damper (UPD) thanks to which a flutter-free design could be achieved.

3.2 Second excitation mode

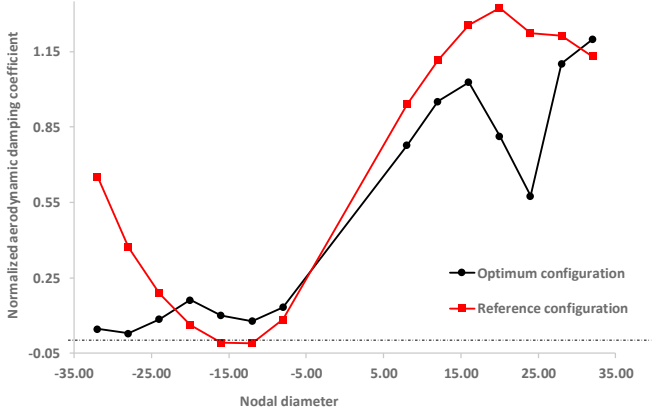

FIGURE 14: FLUTTER STABILITY RESULTS FOR THE SECOND EXCITATION MODE - NOMINAL AND OPTIMAL CONFIGURATIONS

When analyzing the results for the second mode's response, a stable design was obtained since all the aerodynamic damping coefficients are positive, that is, the optimum curve is above the stability limit line (see Figure 14). This indicates that, in terms of the second excitation mode, a flutter-free assembly can be attained.

Finally, it has been found interesting to add the aerodynamic work per cycle of the reference and the optimum configurations for the first and second modes. The area in red represents the zones where the aerodynamic work contribution is higher. In this precise case, as the blade surface is maintained fixed, the difference of the aerodynamic work distributions per cycle between both (reference and optimum configurations) is due to the variation on the structural modes for the considered designs. Figure 15 shows the aerodynamic work distribution in the suction side of the considered configurations.

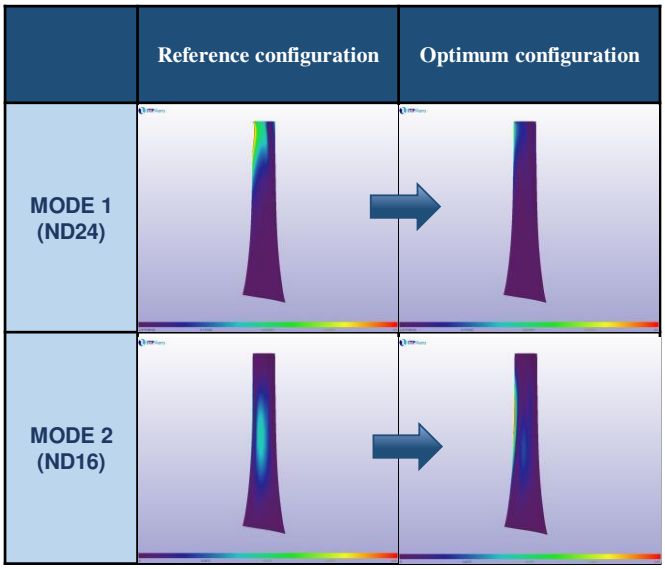

FIGURE 15: AERODYNAMIC WORK PER CYCLE DISTRIBUTION FOR FIRST AND SECOND MODES – NOMINAL AND OPTIMAL CONFIGURATIONS

CONCLUSION

This research aimed at understanding and optimizing the blade interlock mechanism to improve the dynamic behavior of the assembly. For that end, an examination of six different interlock design parameters was performed by means of a Design of Experiment. Accordingly, a dynamic analysis model was prepared, and modal and flutter stability analyses were developed for each of the considered design points.

The main purpose of the modal analysis drew towards identifying the frequencies and the mode shapes for a subsequent flutter analysis, which would provide an aerodynamic damping coefficient that refers to the stability of the system. From this work, it is confirmed that the modal analysis has a significant influence in the flutter stability results. For most of the cases an increase in the modal frequency results in an improved flutter behavior. In short, the parameters that have influence in the modal analysis will also have relevance in flutter stability.

This study has analyzed the dynamic response of the first three excitation modes. Overall, the third mode was stable for all the design points whereas first and second modes were unstable at least for the nominal or reference design point. Obtaining a stable configuration for the second mode was found to be feasible; however, after evaluating the results, a minimum structural damping must be necessary to ensure a flutter-free design for the first mode. The way to create additional structural damping to compensate for the negative aerodynamic damping is by means of inserting friction dampers.

The considered interlock design parameters were the interlock angle, the interlock position, the interlock contact length, the interlock contact height, the knives position and the pretwist angle. The conclusions reached after analyzing the data obtained in this research are summarized below:

• Contrary to what it was anticipated, *interlock angle* showed almost no influence at all neither in the modal analysis nor in the flutter behavior.

• Among all the considered parameters, the *interlock axial position* with respect to the middle of the shroud turns out to be the most relevant parameter for both, modal and flutter analyses. Indeed, moving the interlock contact towards the trailing edge gives the most beneficial results. In a 2D blade profile, it is known that the sensitivity is higher when the torsional axis is located closer to the leading edge, while the blade is gaining stability when the aforementioned axis is in the vicinity of the trailing edge. When working with complex modes and 3D profiles, it has been proven that the interlock position has a stabilization effect, and when this parameter is moved towards the trailing edge, the torsional part of the mode is affected due to the displacement of the torsional axis. Therefore the overall aeroelastic stability of the system is improved.
This goes in line with the results of many other researchers because this concludes that the stability is remarkably sensitive to the exact location of the torsional axis.

• In general, a contact face increase raises the rigidity of the system. In flutter analysis, for the first mode the *interlock contact length* is more relevant, whereas to improve the flutter behavior for the second mode the *interlock contact height* is more influential.

• The effect of the *knives position* was considered almost null at the beginning but after proving the sensitivity of each parameter, knives position plays a crucial part in improving the flutter response of the assembly. As it is the third (for first mode) and the second (for second mode) most influential parameter in the interlock shroud design.

• For *pretwist angle* two differentiated responses have been found. When contact is assured, that is, when the pretwist angle takes values higher than or equal to unity, the parameter has no influence in any of the analyses. On the other hand, when working with too small pretwist angles the contact face is reduced and therefore the design becomes less rigid. This rigidity decrease will create a different behavior in the modes, and in this case, the effect is unfavorable for the first mode and beneficial for the second one. This adverse effect for the first mode is due to that even though the modal and aeroelastic results can be improved for the 24ND; for the rest of them, the responses change abruptly, and the worst case appears at a different ND with an aerodynamic damping value lower than the reference one.

The interdependency of the mentioned parameters was also tested in the parameters sensitivity part and it was concluded that the parameters individually had a higher effect than combined but both effects are noticeable in the results.

Finally, an optimization problem was defined and solved, with the most influential four interlock parameters as the design variables and the absolute value of the negative aerodynamic damping as the objective function to be minimized. The results concluded that, as stated before, a stable design for the second mode is feasible. Upon optimizing the shroud configuration, the results suggest that further improvement of the airfoil would be required to reach the desired flutter-free mechanism.

In brief, this research contributes towards determining the most influential interlock design parameter on the dynamic behavior of a blade-disk assembly and making future recommendations for flutter analysis.

FUTURE WORK

Considerable effort is being made in order to standardize and perfect the flutter behavior analyses. Currently, there are many research works motivating these analyses which are able to create flutter-free blade mechanisms that can prevent flutter damage and are undoubtedly beneficial for the aerospace industry. However, most of the numerical research is focused on cantilever type blades, which does not really predict the tendency of a typical blade with interlock contact. In consequence, using this study as a foundation, future work will focus on reproducing a numerical approximation for the dependency between frequency values, mode shapes and flutter behavior.

This work encompasses the methodology to be followed to examine the influence of some design parameters for a dummy blade but can be generalized for any blade with interlock contact. Therefore, a possible next step may involve a repetition of the process using the same methodology for a real blade design,

other material specifications or different flight operating conditions.

Analyzing the nonlinear structural damping generated by friction interfaces did not fall within the scope of this work but will be a required future line of research, since the interlock contact itself gives additional structural damping to the system. This will contribute to minimize the displacements and to maintain the vibration within negligible values on a possible unstable situation.

The authors believe that as technology keeps evolving, further developments and research are likely to lead to a creation of a flutter-free blade design in a matter of years.

ACKNOWLEDGEMENTS

The authors would like to express their gratitude to ITP Aero for supporting this research and permission to publish the paper.

This work was supported by Cranfield University and the University of Basque Country through an Erasmus+ scholarship, and falls within the framework of an educative collaboration project with Industria de TurboPropulsores (ITP) Aero company. The author also wishes to thank Bizkaiko Foru Aldundia, BBK and Basque Government for financial assistant through their academic excellence programs.

A special consideration is given to Retos Colaboración del Ministerio de Universidades which has financially collaborated with this publication by means of a project called ENVIDIA (Entorno Virtual de Diseño y Fabricación de Turbinas Aeronáuticas).

The permission to publish this paper is gratefully acknowledged.

REFERENCES

[1] Advisory Council for Aeronautics Research in Europe (ACARE), Flightpath 2050, Isbn 978-92-79-19724-6. (2011) 28. https://doi.org/10.2777/50266.

[2] Rolls Royce UltraFan, (2019). https://www.rolls-royce.com/products-and-services/civil-aerospace/future-products.aspx#section-overview.

[3] Safran Aircraft Engines Ultra High Propulsive Efficiency Demonstrator, (2019). https://www.safran-aircraft-engines.com/innovation-0 (accessed October 1, 2019).

[4] J.-F. Brouckaert, F. Mirville, K. Phuah, P. Taferner, Clean Sky research and demonstration programmes for next-generation aircraft engines, Aeronaut. J. 122 (2018) 1163–1175. https://doi.org/10.1017/aer.2018.37.

[5] D. Koyama, Technology Strategy for Future Civil Large Aeroengines, Keynote Speech, in: Japan, 2016.

[6] R. Corral, J.M. Gallardo, C. Martel, A Conceptual Flutter Analysis of a Packet of Vanes Using a Mass-Spring Model, J. Turbomach. 131 (2009). https://doi.org/10.1115/1.2952364.

[7] J. Bijewitz, A. Seitz, M. Hornung, Architectural Comparison of Advanced Ultra-High Bypass Ratio Turbofans for Medium to Long Range Application, in: Deutscher Luft und Raumfahrtkongress, Augsburg, 2014: p. Paper No: 340105.

[8] P.J. Nowinski M., Flutter mechanism in low pressure turbine blades, J. Eng. Gas Turbines Power. 122 (2000) 82–88. https://doi.org/10.1115/1.483179.

[9] J. Panovsky, R.E. Kielb, A Design Method to Prevent Low Pressure Turbine Blade Flutter, Vol. 5 Manuf. Mater. Metall. Ceram. Struct. Dyn. Control. Diagnostics Instrumentation; Educ. 122 (1998) V005T14A052. https://doi.org/10.1115/98-GT-575.

[10] S. Stapelfeldt, M. Vahdati, Improving the Flutter Margin of an Unstable Fan Blade, J. Turbomach. 141 (2019) 071006. https://doi.org/10.1115/1.4042645.

[11] R. Corral, J.M. Gallardo, C. Vasco, Aeroelastic Stability of Welded-in-Pair Low Pressure Turbine Rotor Blades: A Comparative Study Using Linear Methods, J. Turbomach. 129 (2007) 72–83. https://doi.org/10.1115/1.2366512.

[12] A.S. Rangwala, Structural Dynamics of Turbo-Machines, 2009.

[13] M.B. Henderson, D. Arrell, R. Larsson, M. Heobel, G. Marchant, Nickel based superalloy welding practices for industrial gas turbine applications, Sci. Technol. Weld. Join. 9 (2004) 13–21. https://doi.org/10.1179/136217104225017099.

[14] A. Basak, S. Das, Microstructural Characterization of MAR-M247 Fabricated through Scanning Laser Epitaxy, Solid Free. Fabr. Symp. (2017) 448–459.

[15] J.M. Kalinowski, Weldability of a Nickel-Based Superalloy, NASA-CR-195376, Ohio, US, 1994.

[16] R. Corral, J. Crespo, F. Gisbert, Parallel multigrid unstructured method for the solution of the Navier-Stokes equations, AIAA Pap. (2004) 8717–8728. https://doi.org/10.2514/6.2004-761.

[17] R. Corral, F. Gisbert, J. Pueblas, Computation of turbomachinery flows with a parallel unstructured mesh Navier-Stokes equations solver on GPUs, 21st AIAA Comput. Fluid Dyn. Conf. (2013) 24–27. https://doi.org/10.2514/6.2013-2864.

[18] R. Corral, A. Escribano, F. Gisbert, A. Serrano, C. Vasco, Validation of a linear multigrid accelerated unstructured Navier-Stokes solver for the computation of turbine blades on hybrid grids, 9th AIAA/CEAS Aeroacoustics Conf. Exhib. (2003). https://doi.org/10.2514/6.2003-3326.

[19] R.A. Loyola, O.M. Querin, A.G. Jiménez, C.A. Gordoa, A sequential element rejection and admission (SERA) topology optimization code written in Matlab, (2018). https://doi.org/10.1007/s00158-018-1939-x.

[20] A.R. Stäblein, M.H. Hansen, G. Pirrung, Fundamental aeroelastic properties of a bend–twist coupled blade section, J. Fluids Struct. 68 (2017) 72–89. https://doi.org/10.1016/j.jfluidstructs.2016.10.010.

[21] P. Petrie-Repar, V. Makhnov, N. Shabrov, E. Smirnov, S. Galaev, K. Eliseev, Advanced Flutter Analysis of a Long Shrouded Steam Turbine Blade, (2014) V07BT35A022. https://doi.org/10.1115/gt2014-26874.

2021-01-11

Design space exploration of turbine blade shroud interlock for flutter stability

Larrieta, Olatz

American Society of Mechanical Engineers

Larrieta O, Alonso R, Perez Escobar O, et al., (2021) Design space exploration of turbine blade shroud interlock for flutter stability. In: ASME Turbo Expo 2020: Turbomachinery Technical Conference and Exposition, 21-25 September 2020, London, Virtual Event. Paper number GT2020-16040 https://doi.org/10.1115/GT2020-16040